ORIGINAL ARTICLE

Traumatic Brain Injury by a Closed Head Injury Device Induces Cerebral Blood Flow Changes and Microhemorrhages

Srinivasu Kallakuri[1], Sharath Bandaru[1], Nisrine Zakaria[1], Yimin Shen[2], Zhifeng Kou[1,2], Liying Zhang[1], Ewart Mark Haacke[1,2], John M Cavanaugh[1]

[1]Department of Biomedical Engineering, Wayne State University, [2]Department of Radiology, Wayne State University School of Medicine, Detroit, Michigan, USA

Address for correspondence:
Dr. Srinivasu Kallakuri,
Department of Biomedical Engineering, 818 W Hancock, Detroit, Michigan - 48201, USA.
E-mail: skallakuri@wayne.edu

ABSTRACT

Objectives: Traumatic brain injury is a poly-pathology characterized by changes in the cerebral blood flow, inflammation, diffuse axonal, cellular, and vascular injuries. However, studies related to understanding the temporal changes in the cerebral blood flow following traumatic brain injury extending to sub-acute periods are limited. In addition, knowledge related to microhemorrhages, such as their detection, localization, and temporal progression, is important in the evaluation of traumatic brain injury. **Materials and Methods:** Cerebral blood flow changes and microhemorrhages in male Sprague Dawley rats at 4 h, 24 h, 3 days, and 7 days were assessed following a closed head injury induced by the Marmarou impact acceleration device (2 m height, 450 g brass weight). Cerebral blood flow was measured by arterial spin labeling. Microhemorrhages were assessed by susceptibility-weighted imaging and Prussian blue histology. **Results:** Traumatic brain injury rats showed reduced regional and global cerebral blood flow at 4 h and 7 days post-injury. Injured rats showed hemorrhagic lesions in the cortex, corpus callosum, hippocampus, and brainstem in susceptibility-weighted imaging. Injured rats also showed Prussian blue reaction products in both the white and gray matter regions up to 7 days after the injury. These lesions were observed in various areas of the cortex, corpus callosum, hippocampus, thalamus, and midbrain. **Conclusions:** These results suggest that changes in cerebral blood flow and hemorrhagic lesions can persist for sub-acute periods after the initial traumatic insult in an animal model. In addition, microhemorrhages otherwise not seen by susceptibility-weighted imaging are present in diverse regions of the brain. The combination of altered cerebral blood flow and microhemorrhages can potentially be a source of secondary injury changes following traumatic brain injury and may need to be taken into consideration in the long-term care of these cases.

Key words: Arterial spin labeling, cerebral blood flow, hemorrhages, marmarou model, Prussian blue, susceptibility-weighted imaging, traumatic brain injury

Access this article online

Quick Response Code:

Website:
www.clinicalimagingscience.org

DOI:
10.4103/2156-7514.166354

INTRODUCTION

An estimated 1.7 million traumatic brain injuries occur annually in the United States and are attributed to a third of all injury-related deaths and a major cause of disability and cognitive disorders in young adults.[1,2] The pathological sequelae following traumatic brain injury involve a variety of primary and secondary injuries which may continue to evolve from the time of primary injury.[3-5] Alterations in the cerebral blood flow and microhemorrhages are two such secondary injuries whose better understanding may help lead to improved therapeutic opportunities and the ultimate management or prevention of neuronal and functional damage after traumatic brain injury.

Regulation of cerebral blood flow or cerebral autoregulation is complex with multiple overlapping mechanisms and influencing factors.[6-8] Following a traumatic insult, the normal autoregulatory mechanisms are disturbed and can be a factor in the progression of secondary injury changes.[6,9,10] In fact, reduced cerebral blood flow in clinical and experimental traumatic brain injury settings is well known and can contribute to ischemia and brain damage.[10-15] It has been reported that global cerebral blood flow was significantly reduced in traumatic brain injury, with low cerebral blood flow in the first 24 h being associated with poor outcome.[13,16] However, cerebral blood flow changes following closed head injuries are not well studied. The few available experimental studies were limited to measuring cerebral blood flow changes a few hours (30 min–8 h) to 2 days after traumatic brain injury, but not over extended periods after injury. Also, measurements in these studies were limited to one or two anatomical regions with the use of laser Doppler flowmetry probe on a specific location of interest or analyzing limited slices despite using advanced magnetic resonance perfusion imaging techniques such as arterial spin labeling.[11,17-19]

Besides cerebral blood flow, the detection and localization of smaller hemorrhages can provide valuable knowledge on the mechanism of injury as well as prognosis following traumatic brain injury.[20] Detecting small hemorrhages may be helpful in the evaluation of diffuse axonal injury which is commonly associated with small hemorrhages seated deep in the brain, and conventional imaging may not be able to reveal all levels of hemorrhages in the brain. For that matter, focal hemorrhagic lesions in major white matter tracts have been usually associated with microscopic diffuse axonal injury and are routinely used as a diagnostic marker for diffuse axonal injury.[21-23] Also, a significant portion of diffuse axonal injury cases manifest hemorrhagic lesions, but are usually much smaller than extra-axial hematomas and hemorrhagic contusions. Pathological data also shows microhemorrhages at the boundaries of gray matter/white matter, in the corpus callosum, internal capsule, and brainstem.[24] However, studies aimed at finding the temporal progression of microhemorrhages by susceptibility-weighted imaging in an animal model of closed head injury and their histological validation in the same animal model are lacking.

Therefore, the purposes of this study were: (1) To assess the temporal and spatial changes in cerebral blood flow by arterial spin labeling and (2) To assess the presence of microhemorrhages by susceptibility-weighted imaging and their validation by Prussian blue staining in rats subjected to a closed head injury by Marmarou impact acceleration device which is capable of inducing diffuse axonal and vascular injuries.[25-27] Results from this study indicate that a single traumatic insult to the brain induces cerebral blood flow changes as well as microhemorrhages in various brain regions extending to 7 days post-trauma in a rat impact acceleration injury model.

MATERIALS AND METHODS

Surgical procedure and traumatic brain injury induction

All sterile surgical and animal handling procedures in these experiments were approved by the Wayne State University Institutional Animal Care and Use Committee. All rats were administered Buprenex (0.3 mg/kg) subcutaneously 20 min prior to the induction of traumatic brain injury. All rats were anesthetized initially by a mixture of 3% isoflurane and 0.6 l/min oxygen in an anesthesia chamber which was further maintained (1–1.75% isoflurane and 0.6 l/min oxygen) via a nose cone. After ensuing adequate depth of anesthesia, the periosteum was reflected by a midline skin incision to place a steel disc (10 mm diameter and 3 mm thickness) using cyanoacrylate (Elmer's Products, Columbus, OH, USA) between the bregma and lambdoid sutures. Then the rat was positioned prone on a foam bed contained in a Plexiglas box (12 × 12 × 43 cm) and secured in place with its head directly under the lower end of Plexiglas tube of the impactor. Just prior to the induction of trauma, the nose cone supplying anesthesia was removed. Then, a 450 g cylindrical brass weight (18 mm diameter) was dropped from a height of 2 m on to the steel helmet affixed to the exposed skull to induce a severe closed head brain injury.[26,28,29] To avoid a second impact, the Plexiglas box was quickly removed after the impact. Sham rats were subjected to identical experimental procedures sans brain injury.

A total of 40 rats were used as part of these investigations. Cerebral blood flow changes were measured by arterial

spin labeling in 13 anesthetized male Sprague Dawley rats (350–425 g; Harlan, IN, USA) that were randomly assigned to sham (n = 7) and traumatic brain injury (n = 6) groups. These rats were allowed to survive for 7 days and were imaged before and at 4 h, 24 h, 3 days, and 7 days after trauma. These rats were also monitored for this duration to surface right, an indirect measure of loss of consciousness. Traumatic brain injury rats showed significantly prolonged duration to surface right (355 ± 65 s), compared to sham animals (162 ± 25 s).[27,30]

For assessing microhemorrhages by susceptibility-weighted imaging and subsequent Prussian blue staining, a separate set of 27 anesthetized male Sprague Dawley rats were used. These rats were allowed to survive for 4 h (n = 8; imaged at 4 h), 24 h (n = 6; imaged at 4 and 24 h), 3 days (n = 7; imaged at 4 h, 24 h, and 3 days), and 7 days (n = 6; imaged at 4 h, 24 h, 3 days, and 7 days) after trauma.

Arterial spin labeling to assess cerebral blood flow

Pulsed arterial spin labeling measurements were performed using a 7 T horizontal-bore magnetic resonance spectrometer (ClinScan; Bruker, Karlsruhe, Germany) with a 30 cm bore actively shielded gradient coil set capable of producing a gradient strength of up to 290 milliTesla/meter (mT/m) and a slew rate of 1160 T/m/s. For all arterial spin labeling measurements, the rats were initially anesthetized (3% isoflurane and 1 l/min air) and maintained (0.75–1.75% isoflurane and 1 l/min air) via a nose cone for the duration of imaging procedure. Rats were secured with stereotaxic ear bars to minimize movement during scanning with the head aligned at the isocenter of the magnet. A whole-body birdcage radiofrequency coil (inner diameter: 7 cm) was used as the transmitter for homogeneous radio frequency excitation, and a surface coil was used as the receiver, with active radio frequency decoupling to avoid signal interference. The field of view was 35 × 28.44 mm^2 with a matrix size of 128 × 104. The voxel size was 0.273 × 0.273 × 2 mm^3. The arterial spin labeling image acquisition parameters were: Repetition time = 3000 ms, echo time = 16 ms, number of slices = 8, slice thickness = 2 mm, inter-slice gap = 0.5 mm, and number of acquisitions = 50. Eight two-dimensional coronal images covering the entire brain [Figure 1] were obtained for each rat at each time point. First, data from the brainstem region (slices labeled 1–4) [Figure 1a] was acquired and then the grids were moved to acquire data from the cortical regions (slices labeled 5–8) [Figure 1b]. The pulsed arterial spin labeling sequence with echo planar imaging readout (Bruker/Siemens sequence named-Picore Q2TIPS) was used to measure cerebral blood flow.[31,32]
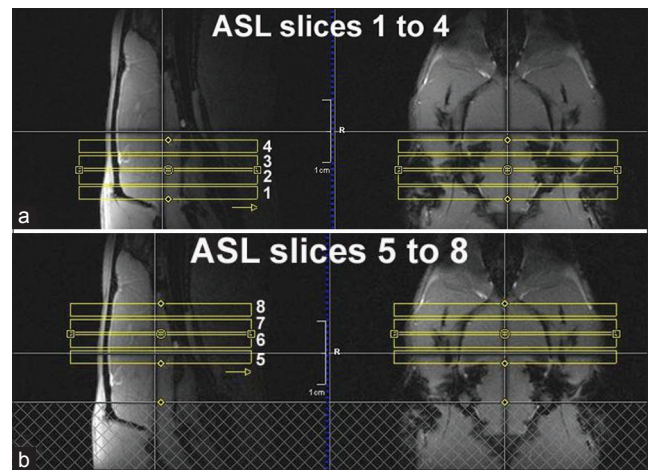

Figure 1: Sagittal and axial magnetic resonance localizer images show the slice locations of arterial spin labeling imaging in a typical male Sprague Dawley rat used in this study. (a) Slices numbered 1–4 covered brainstem regions and (b) slices numbered 5–8 covered cortical regions.

Susceptibility-weighted imaging to assess hemorrhages

For susceptibility-weighted imaging, rats were placed in a 4.7 Tesla horizontal-bore magnetic resonance spectrometer (AVANCE; Bruker, Karlsruhe, Germany) with a 72 mm bore actively shielded gradient coil capable of producing a gradient strength of up to 250 mT/m. The field of view was set at 40 × 40 × 24 mm^3 to image the whole brain. The imaging parameters were as follows: repetition time = 36 ms, echo time = 15 ms, flip angle = 20°, with an image matrix size of Nx × Ny × Nz = 512 × 512 × 24 image matrix size, and number of acquisitions = 2. Susceptibility-weighted imaging is based on a fully flow-compensated, high-resolution, three-dimensional gradient echo method.[33] The flow compensation ensures that there is no flow-induced phase in the susceptibility-weighted imaging filtered phase images.

Arterial spin labeling image analysis

The cerebral blood flow maps generated by the arterial spin labeling were processed using signal processing in nuclear magnetic resonance software (SPIN version 2045, http://www.mrc.wayne.edu/). The arterial spin labeling image [Figure 2] was amplified to accurately delineate a region of interest using the polygon selection in signal processing in nuclear magnetic resonance software.

Cerebral blood flow changes in various regions, termed regional cerebral blood flow, encompassing parietal cortex (right parietal cortex, left parietal cortex, average of left and right parietal cortex), striatum (right striatum, left striatum, average of left and right striatum), hippocampus (right hippocampus, left hippocampus,
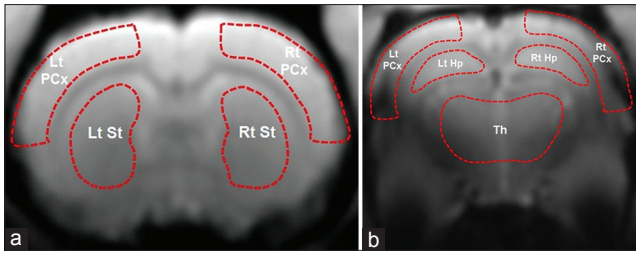
Figure 2: (a and b) Manual drawings of regions of interest on arterial spin labeling images in coronal view of the brain of a typical male Sprague Dawley rat used in this study. Red dashed lines indicate regions of interest for measuring cerebral blood flow in the cortical and sub-cortical regions (Lt PCx = Left parietal cortex; Rt PCx = Right parietal cortex; Lt Hp = Left hippocampus; Rt Hp = Right hippocampus; Th = Thalamus; Lt St = Left striatum; Rt St = Right striatum).

Figure 3: Manual drawings of regions of interest on arterial spin labeling images in coronal view of the brain of a typical male Sprague Dawley rat used in this study. Red dashed lines indicate regions of interest for brainstem (Bs) in three different slices (a-c) for measuring cerebral blood flow.

average of left and right hippocampus), bilateral thalamus [Figure 2], and brainstem [Figure 3] were measured by drawing regions of interest around specific brain regions using corresponding images in the rat brain atlas as a guide.[34] Average cerebral blood flow values from all these locations were used to calculate a combined regional cerebral blood flow. Average global cerebral blood flow was also measured by drawing a single region of interest around the complete brain in each of the eight arterial spin labeling slices. For each group of rats (sham and trauma) at any given time point, cerebral blood flow values obtained from a given brain region from all the rats in that group were averaged to represent the mean cerebral blood flow value for that region.

All data were analyzed for statistical significance using Statistical Package for the Social Sciences (version 20; IBM Corporation, USA). Cerebral blood flow values were expressed as the mean value ± standard error of the mean. Reliability of the data at each time point for all the rats combined was tested (Cronbach's alpha test) with an alpha value ≥ 0.7 being considered as reliable. Group-wise differences were analyzed by repeated measures of analysis of variance. Data was further analyzed for within-group differences by one-way analysis of variance using least significant difference *post-hoc*.

Identification of hemorrhagic lesions in susceptibility-weighted images

In susceptibility-weighted images, hemorrhagic lesions were defined as predominantly hypointense foci that were not compatible with vascular, bone, or artifactual structures in conventional T2 and susceptibility-weighted images and by our slice-by-slice comparison with pre-trauma images of the same animal. For locating hemorrhages in susceptibility-weighted images, coronal slices encompassing the entire corpus callosum, the surrounding cortical and sub-cortical areas, as well as the brainstem areas were investigated. Selective images
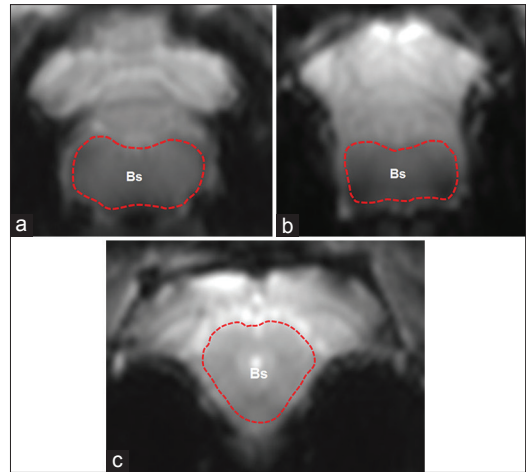
showing putative hypointense areas were then compared with the corresponding histological sections for the presence of Prussian blue reaction products in the same area as highlighted by susceptibility-weighted images.

Termination and fixation for Prussian blue histology

At the conclusion of their respective post-injury susceptibility-weighted imaging, each rat was euthanized (sodium pentobarbital 60 mg/kg) and transcardially perfused with cold 4% paraformaldehyde in phosphate-buffered saline. The brain was fixed in 4% paraformaldehyde with 20% sucrose. The cerebral hemispheres encompassing midbrain were cut into 40 μm frozen coronal sections (Leica CM 3050; Leica Microsystems Nussloch GmbH, Nussloch, Germany) and collected free floating in phosphate-buffered saline filled multi-well plates.

Prussian blue histochemistry

For Prussian blue analysis, a total of 22 brains (4 h, $n = 6$; 24 h, $n = 4$; 3 days, $n = 7$; 7 days, $n = 3$; control, $n = 2$) were used. A series of representative coronal brain sections (average of 10 sections per rat) encompassing the anterior to posterior regions of cortex including the brainstem at the level of midbrain were stained. For staining, the sections were washed in 1× phosphate-buffered saline solution and immersed for 45 min in a solution of equal parts of freshly prepared 20% aqueous hydrochloric acid and 10% potassium ferrocyanide. Then, the sections were rinsed in distilled water, counterstained in nuclear fast red solution for 5 min, and rinsed further in distilled water to remove any staining artifacts. These sections were subsequently dehydrated in graded alcohol and cleared in three changes of xylene and cover-slipped with Permount.

RESULTS

Cerebral blood flow changes in sham rats

In sham rats, no significant differences were observed in cerebral blood flow values of parietal cortex, striatum, hippocampus, thalamus, and brainstem before sham surgery and at various post-sham survival periods, with the flow values remaining stable over the measured periods [Figure 4a–d]. Also, no differences were observed within the combined regional and global cerebral blood flow levels at all the measured time points in sham rats [Figure 4e].

Cerebral blood flow changes in traumatic brain injured rats

In the parietal cortex, hippocampus and striatum of injured rats, the values of cerebral blood flow decreased significantly by 7 days post-injury compared to their respective pre-injury levels [Figure 5]. Furthermore, the decrease in
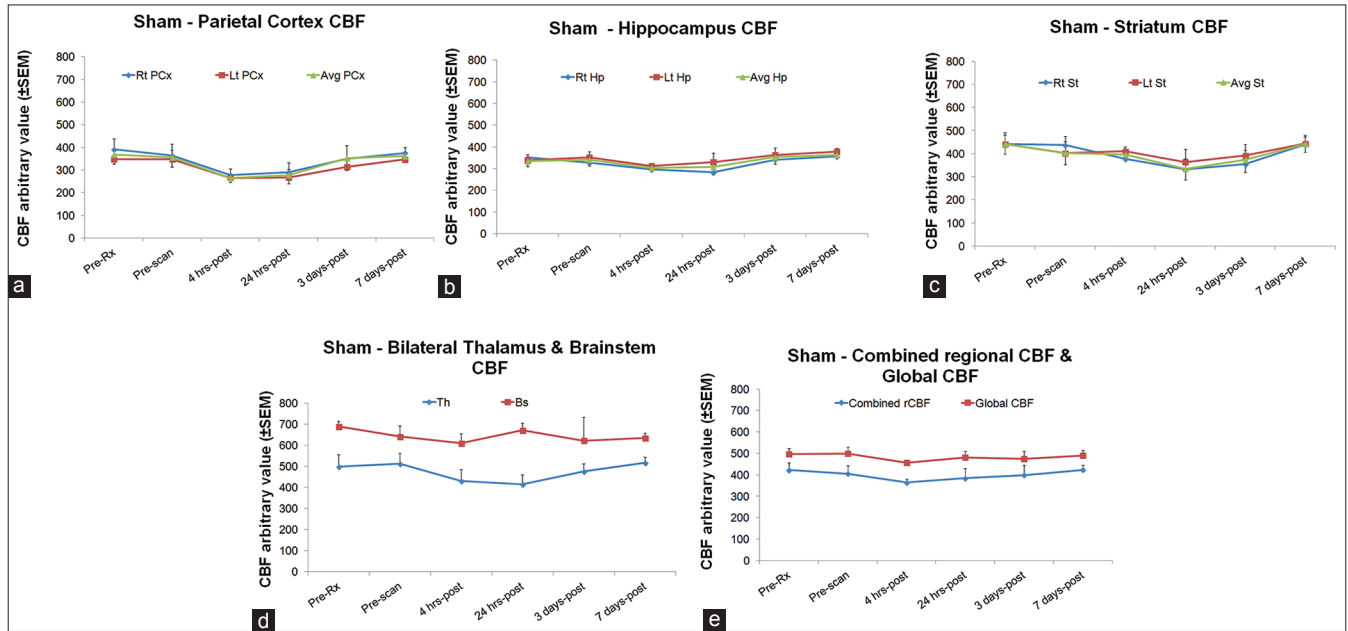

Figure 4: (a-e) Charts show temporal cerebral blood flow changes in different brain regions of sham rats. In sham rats, no apparent differences were observed in the cerebral blood flow (CBF) values at various time points in the structures analyzed.
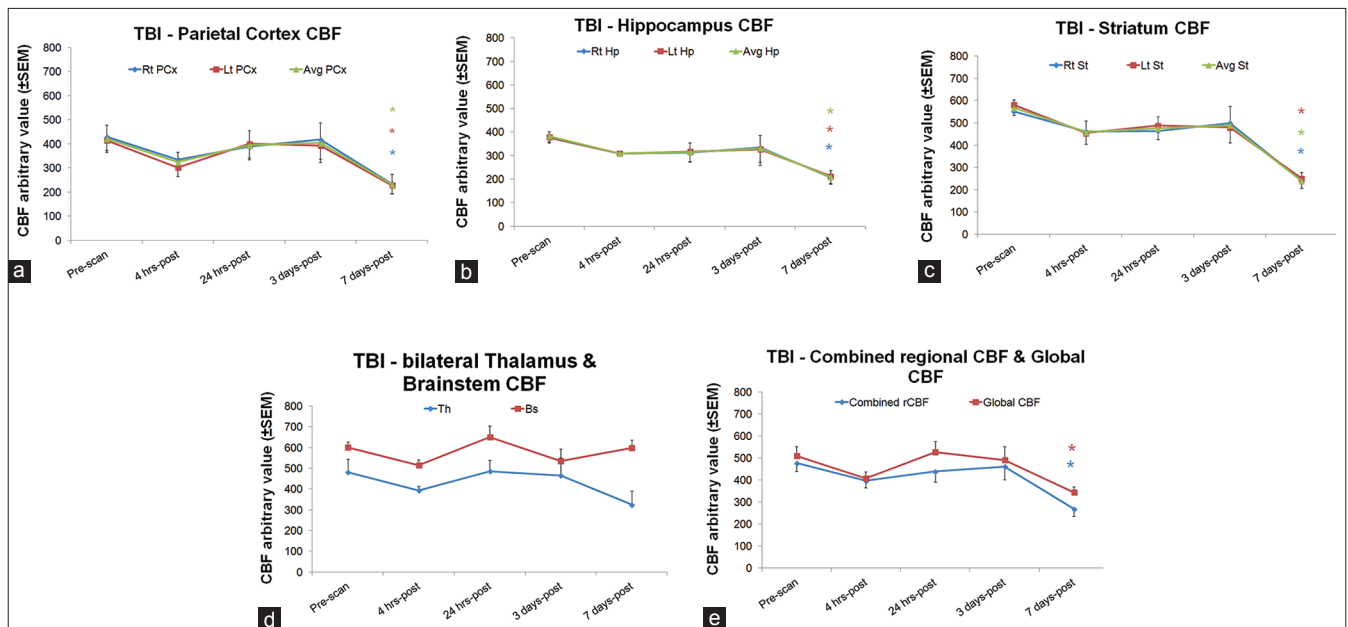
Figure 5: Traumatic brain injury (TBI) induced temporal cerebral blood flow (CBF) changes. Cerebral blood flow 7 days post-trauma was significantly low in (a) parietal cortex and (b) hippocampus, compared to pre-injury, 24 h and 3 days post-injury. Values in (c) striatum at 7 days post-trauma were significantly low compared to the values at pre-injury and all post-trauma periods. (d) Cerebral blood flow values in thalamus and brainstem showed no changes. (e) Combined regional and global cerebral blood flow was significantly reduced 7 days post-trauma compared to their pre-injury, 24 h, and 3 days post-injury levels. (*$P<0.05$; SEM = Standard error of the mean).

cerebral blood flow value of parietal cortex [Figure 5a] and hippocampus [Figure 5b] at 7 days post-trauma was significantly low, compared to their levels at 24 h and 3 days post-trauma ($P < 0.05$). In striatum [Figure 5c], the cerebral blood flow value decreased significantly at 7 days compared to the values at all other post-trauma survival periods ($P < 0.05$). In the case of thalamus, an insignificant decrease in cerebral blood flow value was observed at 7 days post-trauma [Figure 5d]. Brainstem showed no significant changes in cerebral blood flow values except for some insignificant decreases at 4 h and 3 days post-trauma [Figure 5d]. An analysis of combined regional and global cerebral blood flow values of injured rats also revealed a significant reduction in combined regional and global cerebral blood flow at 7 days post-trauma [Figure 5e] compared to their pre-trauma as well as post-injury 24 h and 3 days levels ($P < 0.05$).

Susceptibility-weighted image analysis of traumatic brain injured rats

Hemorrhagic lesions evidenced as hypointense areas were present in susceptibility-weighted images from a number of rats, encompassing various post-trauma survival periods. Occurrence of these hypointense regions was more frequent in the corpus callosum and the septal nucleus than in other brain regions [Table 1]. In some cases, these hypointense regions in the corpus callosum that appeared 4 h after trauma were not seen a day after trauma, but reappeared at 3 days and 7 days after trauma. Also, in all the rats that survived for 7 days post-trauma, the hypointense region in the septal nucleus close to ventricles appeared to enhance with increasing survival period. In fact, frank hemorrhages in corpus callosum not seen very obviously by T2 imaging [Figure 6a and a'] were prominently exposed by susceptibility-weighted

imaging [Figure 6b', solid arrow]. The susceptibility-weighted image [Figure 6b'] shows putative hypointense areas (arrows) not visible before trauma [Figure 6b]. The hypointense areas appeared to extend beyond the corpus callosum into the adjoining cortex. These observed lesions were also validated histologically as revealed by well-stained Prussian blue streaks in the corresponding location [Figure 6c].

Prussian blue histochemistry

Prussian blue stained regions were observed in sections from all the time points [Table 2]. Prussian blue streaks were observed in various areas of the cortex, sub-cortical structures (striatum, hippocampus, thalamus), white matter tracts (cingulum, corpus callosum, external capsule, fimbria, ventral hippocampal commissure, optic radiations), and midbrain regions (superior and inferior colliculi, substantia nigra, tegmentum, region close to the posterior commissure).

In the sensory-motor cortex, Prussian blue stained streaks were seen extending to various layers and were predominantly located away from the blood vessels but close to the exterior of blood vessels [Figure 7a and b]. Prussian blue stained areas were also found

Table 1: A summary of number of animals with lesions in various brain regions as revealed by SWI				
% Animals with brain lesions shown by SWI	4 h post-TBI ($n = 24$) (%)	24 h post-TBI ($n = 18$) (%)	3-4 days post-TBI ($n = 12$) (%)	7 days post-TBI ($n = 6$) (%)
Cortex	(1/24) 4.2	(1/18) 5.5	(1/12) 8.3	-
Corpus callosum	(8/24) 33.3	(6/18) 33.3	(4/12) 33.3	(2/6) 33.3
Septal nucleus close to ventricles	(1/24) 4.2	(4/18) 22.2	(6/12) 50	(6/6) 100
Hippocampus	(1/24) 4.2	-	-	-
Brainstem	(1/24) 4.2	(2/18) 11.1	(2/12) 16.6	-

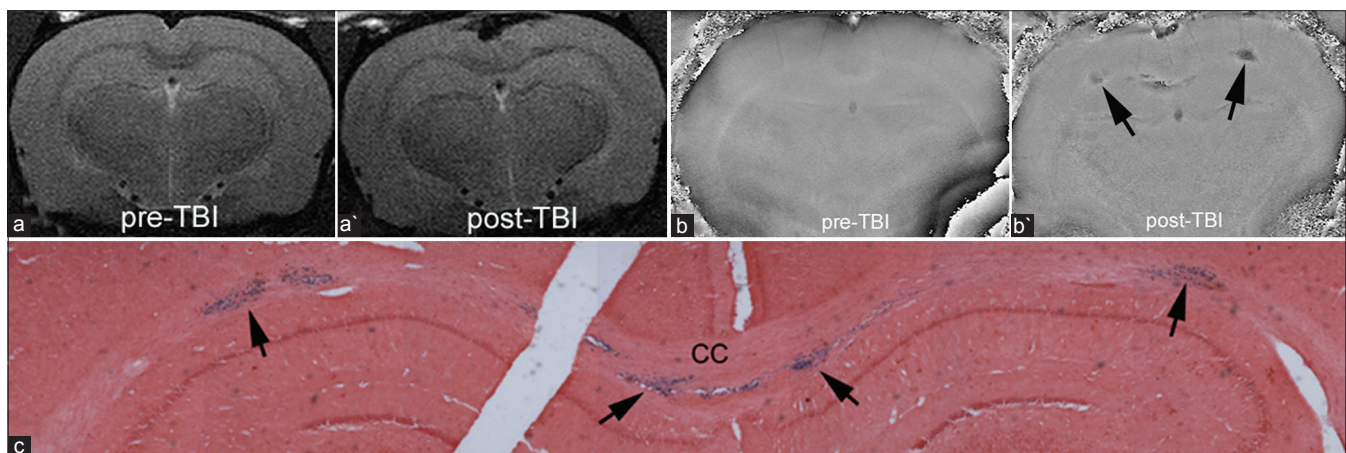SWI: Susceptibility-weighted imaging, TBI: Traumatic brain injury

Figure 6: Comparative pre- and post-trauma T2 and susceptibility-weighted coronal images show lesions in corpus callosum from a rat subjected to traumatic brain injury. (a) Pre-injury T2 image. (a') the corresponding 3-day post-injury T2 image shows no obvious lesion(s) in the corpus callosum. (b) Pre-injury susceptibility-weighted image. (b') The corresponding 3-day post-injury susceptibility-weighted image showing prominent bilateral lesions in the corpus callosum (arrows). (c) Composite image of the Prussian blue stained section shows corresponding reaction products in locations (arrows) that match with findings in the corresponding susceptibility-weighted image.

Table 2: A summary of total number of rats showing microhemorrhagic lesions identified by Prussian blue staining in various brain structures at various survival periods post traumatic brain injury

| Prussian blue locations	6 h post-TBI ($n=6$) (%)	24 h post-TBI ($n=4$) (%)	3-4 days post-TBI ($n=7$) (%)	7 days post-TBI ($n=3$) (%)	Control ($n=2$)
Cortex	4/6 (66.6)	4/4 (100)	3/7 (42.8)	1/3 (33.3)	-
Cingulum	1/6 (16.6)	-	2/7 (28.5)	-	-
Corpus callosum	4/6 (66.6)	3/4 (75)	6/7 (85.7)	2/3 (66.6)	-
Corpus callosum (forceps major)	4/6 (66.6)	-	1/7 (14.2)	-	-
Ventricles	4/6 (66.6)	3/4 (75)	5/7 (71.4)	3/3 (100)	-
Striatum	-	1/4 (25)	2/7 (28.5)	1/3 (33.3)	-
Septal nucleus	-	1/4 (25)	1/7 (14.2)	1/3 (33.3)	-
Anterior commissure	-	-	2/7 (28.5)	1/3 (33.3)	-
Optic chiasm	-	-	-	1/3 (33.3)	-
Alveus	1/6 (16.6)	1/4 (25)	1/7 (14.2)	1/3 (33.3)	-
Fimbria	1/6 (16.6)	2/4 (50)	3/7 (42.8)	1/3 (33.3)	-
Ventral hippocampal commissure	-	1/4 (25)	-	1/3 (33.3)	-
Hippocampus	4/6 (66.6)	2/4 (50)	5/7 (71.4)	2/3 (66.6)	-
Thalamus	2/6 (33.3)	1/4 (25)	3/7 (42.8)	2/3 (66.6)	-
Optic tracts	1/6 (16.6)	-	3/7 (42.8)	1/3 (33.3)	-
External capsule	2/6 (33.3)	3/4 (75)	3/7 (42.8)	2/3 (66.6)	-
Internal capsule	-	1/4	-	1/3	-
Midbrain	2/6 (33.3)	1/4 (25)	4/7 (57)	2/3 (66.6)	-

TBI: Traumatic brain injury
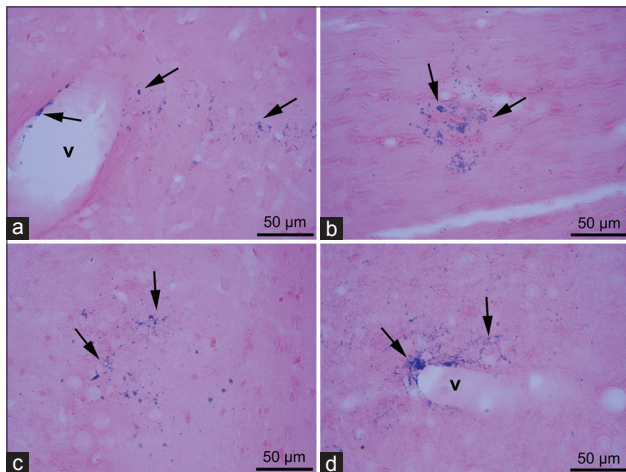
Figure 7: Representative images show Prussian blue reaction products in various brain regions of a rat 24 h after traumatic brain injury. (a) Prominent Prussian blue reaction products (arrows) extending into the cortical region away from a blood vessel (v) and in the lumen of the vessel. (b) Prussian blue reaction product (arrows) in the corpus callosum with clear adjacent capillaries. (c) Prussian blue reaction product (arrow) in the cornu ammonis region of hippocampus. Clear hippocampal blood vessels can be seen in the vicinity. (d) Prominent Prussian blue reaction product (arrows) dispersion in the thalamic region. The blood vessel (v) with its lumen stained blue can be seen.

in the neuropil close to the pia, where many cortical penetrating vessels could be seen. In the corpus callosum, the blood vessels appeared to be particularly vulnerable to rupture, resulting in extravasation of erythrocytes into the adjacent cortex and axonal tracts or remaining in close association with the exterior of the ruptured vessels. In some cases, these ruptured blood vessels were marked by the appearance of a disrupted endothelial cell layer. A rostral-to-caudal observation of various coronal sections of the injured brains showed the presence of the vascular lesions extending caudally into the forceps major. Furthermore, prominent Prussian blue streaks independent of blood vessels were observed in these regions.

In the hippocampus, blue stained regions were observed in the dorsal hippocampus [Figure 7c] and associated structures such as the dorsal and ventral hippocampal commissure, alveus, cornu ammonis, dentate gyrus, and the fimbria. The blue staining could be seen in the lumen of small blood vessels associated with the hippocampal tissue, as well as around the hippocampal fissure, a site of penetrating blood vessels.

Additional Prussian blue stained regions were observed in the optic tract, thalamic regions [Figure 7d], and areas of the basal ganglia. In the midbrain, areas around the medial geniculate nucleus and the commissure of superior colliculus also showed positive Prussian blue staining. In sections from uninjured rats, no such Prussian blue reaction products could be seen in the cortex, corpus callosum, and other regions.

DISCUSSION

One striking feature of this study is the reproducibility of the observed arterial spin labeling values as confirmed in the sham rats that were imaged twice over a 21-day period before sham surgery, with no significant changes between these two time points in any of the brain regions analyzed. Temporally, the cerebral blood flow values post sham surgery in various brain regions were no different compared to their pre-sham surgery levels.

Our study attempted to show cerebral blood flow changes over a 7-day period in the cortical, sub-cortical, and

brainstem regions, unlike the few available studies that focused on these changes in the cortical regions alone and for only a few hours post-injury.[17-19] Using a 450 g impactor dropped from 2 m, Ito et al., observed a severe elevation in intracranial pressure resulting in reduced cerebral blood flow (<30% of control value) in the cortex 2 h post-trauma.[17] Whereas Prat et al., demonstrated a decrease in cerebral blood flow from 4 h to 8 h after trauma, but not during the initial 3-h period post-trauma induced by dropping a 450 g weight from 1 m which induces a mild injury.[18] In a separate study, Petrov et al., using a similar trauma model, reported a decrease in the cerebral blood flow by 2–3 h after trauma that showed a trend toward normalization by 4 h post-trauma.[19]

Shen et al., using magnetic resonance imaging based perfusion imaging in a similar trauma model, reported reduced hippocampal cerebral blood flow at 4 h (8–14%), 24 h (8%), and 48 h post-trauma (18%), compared to their pre-injury levels. Such hippocampal cerebral blood flow reductions at 4 h (19%) and 24 h (17%) post-trauma were also observed in the current study. Shen et al., also reported cerebral blood flow reductions in parietal cortex measured from one slice at 4 h (~26%), 24 h (23%), and 48 h (17%) post-trauma.[11] In the current study, a reduction in the blood flow of parietal cortex at 4 h post-trauma (23%) with putative recovery by 24 h (only 6% reduction) and 3 days post-trauma (4% reduction) was observed.

Our study demonstrated that sub-cortical regions such as the hippocampus, striatum, and thalamus were also affected following trauma with no apparent changes observed in the brainstem. This variation in regional cerebral blood flow between cortical regions and brainstem may be related to the site of the impact with the helmet being placed between bregma and lambda. Our study showed a significant reduction in the cerebral blood flow of cortical and sub-cortical regions 7 days post-trauma (~49%) compared to their pre-trauma as well as 24 h and 3 days post-trauma levels.

The combined regional cerebral blood flow which included the brainstem also showed an insignificant reduction of about 16% compared to baseline at 4 h post-injury and a significant reduction of ~44% compared to baseline at 7 days post-trauma. Global cerebral blood flow also showed an insignificant reduction of about 20% compared to baseline at 4 h post-trauma and a significant reduction of ~ 32% at 7 days post-trauma. It was previously reported that reduction in cerebral blood flow in the first few hours after injury may reach ischemic levels. In humans, ischemic cell death has been observed in 30% of all traumatic brain injury cases within the first 6 h after injury and was found to cause early death.[35,36] This decreased cerebral blood flow may even trigger secondary injury events. Also, cerebral ischemia has been observed in around 90% of the patients who die following traumatic brain injury.[37] However, the occurrence of ischemic cell death at 7 days post-trauma in this study warrants further investigation, and thus, a mechanistic understanding of the observed blood flow changes may help better manage secondary injury changes.

We postulate the role of an impaired cerebral autoregulation as one of the reasons for the observed abnormal cerebral blood flow changes that can manifest for extended periods after the initial insult. Although not studied, another potential reason for the observed reduced blood flow at 7 days post-trauma may be related to the progressive edematous changes which this model is known to induce.[25,38] Foda and Marmarou reported two forms of brain edema, namely, pericapillary edema in the supraventricular cortical areas underneath the impact site and widening of extracellular space in the corpus callsoum. The lumina of many capillaries were reported to be disfigured and narrowed by vasoconstriction, which indicated that the brain edema in the severely injured rats lasted for longer periods than those injured mildly.[25] In fact, selective inhibition of endothelin-1, a potent vasoconstrictor, in a closed head brain injury model was shown to reduce neurological deficits and edema.[39] Clinically, improved cerebral blood flow following decompressive craniotomy to relieve edema following traumatic brain injury was also reported.[40] Thus, additional studies directed at understanding the blood flow changes at chronic time periods after trauma and the potential role of vasodynamic agents in improving blood flow are needed.

Besides altered cerebral blood flow changes, microhemorrhages following traumatic brain injury could be contributing to the ensuing secondary injury changes in the form of hemorrhagic lesions, as shown in this study by susceptibility-weighted imaging and Prussian blue staining up to 7 days after trauma. Furthermore, the number of microhemorrhages revealed by Prussian blue staining was higher than that revealed by susceptibility-weighted imaging. That all hemorrhages could not be detected by susceptibility-weighted imaging may be related to the evolution of these hemorrhages that may appear at various time points after trauma. This was especially revealed by hypointense areas in the septal nucleus close to ventricles, which appeared to enhance with increasing survival period. This study limited its focus to the presence of microhemorrhages in the cortex and various sub-cortical structures, which are the same regions

that showed altered cerebral blood flow changes. In the cortex, the hemorrhagic products could be observed with no preferential localization. In fact, there appeared to be a preponderance of sub-cortical lesions than cortical lesions. In the corpus callosum, Prussian blue streaks could be observed predominantly in the most posterior sections including the area of forceps major. Corpus callosum is the most common location that showed highest percentage of lesions at all post-trauma time points and our recent investigations also support the presence of extensive diffuse axonal injury in the corpus callosum.[26,41]

The present study also demonstrated prominent Prussian blue hemorrhagic lesions in the hippocampus, which may be related to alterations in cognitive function with additional reaction products being observed in external capsule, optic tracts, fimbria, alveus, and thalamic regions. The detection of these hemorrhages may have potential clinical implications. For example, in the radiological diagnosis of traumatic brain injury patients, the presence of hemorrhages on advanced magnetic resonance imaging and their absence on conventional imaging may have significant clinical impact. Especially in mild traumatic brain injury patients, the presence of hemorrhage will classify them into the category of "complicated mild traumatic brain injury" and they tend to have long-term neurocognitive sequelae. Although we were able to demonstrate hemorrhages extending to 7 days after injury, we were limited in offering specific insights into the temporal progression of the observed hemorrhages as well as their role if any on the observed blood flow changes. The presence of focal and relatively large lesions in corpus callosum and their validation by susceptibility-weighted imaging in the present study supports the role of such lesions in white matter tracts as a diagnostic marker of diffuse axonal injury.[23] Tong et al. (2004), utilizing susceptibility-weighted imaging, reported fewer hemorrhages and lower volume in children with normal outcomes or mild disability than in those moderately or severely disabled after traumatic brain injury, supporting the need for a better detection of hemorrhages.[42]

What are the potential pathological implications of these hemorrhages that can give rise to various extracellular breakdown products of hemoglobin and other hematoproteins of which heme (ferroprotoporphyrin IX) is a crucial player in oxidative stress and tissue injury?[43] Hua et al., (2006) demonstrated brain atrophy in the caudate with prolonged neurological deficits detectable 3 months after an experimentally induced intracerebral hemorrhage.[44] Iron-induced oxidative deoxyribonucleic acid damage in brain injury was shown by Nakamura et al. (2006), who demonstrated enhanced deoxyribonucleic acid polymerase I-mediated biotin-deoxyadenosine triphosphate nick translation and dinitrophenyl signals following infusion of autologous whole blood or ferrous chloride into the right basal ganglia in rats.[45] Furthermore, studies by Regan and Panter (1996) on murine cortical cell cultures have shown that non-toxic concentrations of hemoglobin potentiated neurotoxic effects of synthetic glutamate receptor agonists α-amino-3-hydroxy-5-methyl-4-isoxazolepropionic-acid and kainite, as evidenced by neuronal loss that was attenuated by the addition of iron chelator.[46]

Limitations

Although this study showed changes related to cerebral blood flow and microhemorrhages in a rat model of the impact acceleration injury using a combination of advanced imaging and histology, it had some limitations. For example, the extent of cerebral blood flow changes and microhemorrhages at more chronic time periods is not known. Susceptibility-weighted imaging was able to reveal only a subset of hemorrhages, whereas Prussian blue staining showed many microhemorrhages in diverse cortical and sub-cortical regions that otherwise could not be detected. In order to further improve detecting smaller amounts of iron by susceptibility-weighted imaging, a better signal-to-noise ratio is needed. Finally, in this study, evidence is lacking for any behavioral and cellular injury changes that can be attributed to the observed findings. Future studies can address cellular injury changes, blood flow changes at chronic time periods, and apply therapeutic interventions to alleviate the altered cerebral blood flow.

CONCLUSIONS

Results from this study suggest that a single insult of traumatic brain injury induces cerebral blood flow changes at 4 h and 7 days post-injury in a rat impact acceleration injury model. The model also induces microhemorrhages, visible at various post-injury survival periods in diverse brain locations. Taken together, these findings point to the manifestation of putative injury changes in the brain long after the initial traumatic insult. These ongoing injury changes have potential clinical implications in the overall evaluation and management of traumatic brain injury cases.

Conflicts of interest

There are no conflicts of interest.

REFERENCES

1. Faul M, Xu L, Wald MM, Coronado VG. Traumatic Brain Injury in the United States: Emergency Department Visits, Hospitalizations and Deaths 2002-2006. Atlanta (GA): Centers for Disease Control and Prevention, National Center for Injury Prevention and Control; 2010. p. 1-74.
2. Cossa FM, Fabiani M. Attention in closed head injury: A critical review. Ital J Neurol Sci 1999;20:145-53.
3. Graham DI, McIntosh TK, Maxwell WL, Nicoll JA. Recent advances in neurotrauma. J Neuropathol Exp Neurol 2000;59:641-51.
4. Kumar A, Loane DJ. Neuroinflammation after traumatic brain injury: Opportunities for therapeutic intervention. Brain Behav Immun 2012;26:1191-201.
5. Li W, Dai S, An J, Li P, Chen X, Xiong R, et al. Chronic but not acute treatment with caffeine attenuates traumatic brain injury in the mouse cortical impact model. Neuroscience 2008;151:1198-207.
6. Rangel-Castilla L, Gasco J, Nauta HJ, Okonkwo DO, Robertson CS. Cerebral pressure autoregulation in traumatic brain injury. Neurosurg Focus 2008;25:E7.
7. Peterson EC, Wang Z, Britz G. Regulation of cerebral blood flow. Int J Vasc Med 2011;2011:823525.
8. Zauner A, Muizelaar JP. Brain metabolism and cerebral blood flow. In: Reilly P, Bullock R, editors. Head Injury, London: Chapman and Hall; 1997. p. 89-99.
9. Kennedy DO, Haskell CF. Cerebral blood flow and behavioural effects of caffeine in habitual and non-habitual consumers of caffeine: A near infrared spectroscopy study. Biol Psychol 2011;86:298-306.
10. Sedlacik J, Helm K, Rauscher A, Stadler J, Mentzel HJ, Reichenbach JR. Investigations on the effect of caffeine on cerebral venous vessel contrast by using susceptibility-weighted imaging (SWI) at 1.5, 3 and 7 T. Neuroimage 2008;40:11-8.
11. Shen Y, Kou Z, Kreipke CW, Petrov T, Hu J, Haacke EM. *In vivo* measurement of tissue damage, oxygen saturation changes and blood flow changes after experimental traumatic brain injury in rats using susceptibility weighted imaging. Magn Reson Imaging 2007;25:219-27.
12. Yuan XQ, Prough DS, Smith TL, Dewitt DS. The effects of traumatic brain injury on regional cerebral blood flow in rats. J Neurotrauma 1988;5:289-301.
13. Marion DW, Darby J, Yonas H. Acute regional cerebral blood flow changes caused by severe head injuries. J Neurosurg 1991;74:407-14.
14. Ngai AC, Coyne EF, Meno JR, West GA, Winn HR. Receptor subtypes mediating adenosine-induced dilation of cerebral arterioles. Am J Physiol Heart Circ Physiol 2001;280:H2329-35.
15. Graham DI, Adams JH, Doyle D. Ischaemic brain damage in fatal non-missile head injuries. J Neurol Sci 1978;39:213-34.
16. Barclay L, Zemcov A, Reichert W, Blass JP. Cerebral blood flow decrements in chronic head injury syndrome. Biol Psychiatry 1985;20:146-57.
17. Ito J, Marmarou A, Barzo P, Fatouros P, Corwin F. Characterization of edema by diffusion-weighted imaging in experimental traumatic brain injury. J Neurosurg 1996;84:97-103.
18. Prat R, Markiv V, Dujovny M, Misra M. Evaluation of cerebral autoregulation following diffuse brain injury in rats. Neurol Res 1997;19:393-402.
19. Petrov T, Rafols JA. Acute alterations of endothelin-1 and iNOS expression and control of the brain microcirculation after head trauma. Neurol Res 2001;23:139-43.
20. Tong KA, Ashwal S, Obenaus A, Nickerson JP, Kido D, Haacke EM. Susceptibility-weighted MR imaging: A review of clinical applications in children. AJNR Am J Neuroradiol 2008;29:9-17.
21. Adams JH, Graham DI, Murray LS, Scott G. Diffuse axonal injury due to nonmissile head injury in humans: An analysis of 45 cases. Ann Neurol 1982;12:557-63.
22. Adams JH, Doyle D, Ford I, Gennarelli TA, Graham DI, McLellan DR. Diffuse axonal injury in head injury: Definition, diagnosis and grading. Histopathology 1989;15:49-59.
23. Grossman RI, Yousem DM. Neuroradiology. The Requisites. Philadelphia: Mosby; 2003.
24. Meythaler JM, Peduzzi JD, Eleftheriou E, Novack TA. Current concepts: Diffuse axonal injury-associated traumatic brain injury. Arch Phys Med Rehabil 2001;82:1461-71.
25. Foda MA, Marmarou A. A new model of diffuse brain injury in rats. Part II: Morphological characterization. J Neurosurg 1994;80:301-13.
26. Kallakuri S, Li Y, Zhou R, Bandaru S, Zakaria N, Zhang L, et al. Impaired axoplasmic transport is the dominant injury induced by an impact acceleration injury device: An analysis of traumatic axonal injury in pyramidal tract and corpus callosum of rats. Brain Res 2012;1452:29-38.
27. Li Y, Zhang L, Kallakuri S, Zhou B, Cavanaugh JM. Injury predictors for traumatic axonal injury in a rodent head impact acceleration model. Stapp Car Crash J 2011;55:25-47.
28. Marmarou A, Foda MA, van den Brink W, Campbell J, Kita H, Demetriadou K. A new model of diffuse brain injury in rats. Part I: Pathophysiology and biomechanics. J Neurosurg 1994;80:291-300.
29. Kallakuri S, Cavanaugh JM, Ozaktay AC, Takebayashi T. The effect of varying impact energy on diffuse axonal injury in the rat brain: A preliminary study. Exp Brain Res 2003;148:419-24.
30. Adams J. Methods in behavioral teratology. In: Riley EP, Vorhees CV, editors. Handbook of Behavioral Teratology. New York: Plenum Press; 1986. p. 67.
31. Luh WM, Wong EC, Bandettini PA, Hyde JS. QUIPSS II with thin-slice TI1 periodic saturation: A method for improving accuracy of quantitative perfusion imaging using pulsed arterial spin labeling. Magn Reson Med 1999;41:1246-54.
32. Wang J, Licht DJ, Jahng GH, Liu CS, Rubin JT, Haselgrove J, et al. Pediatric perfusion imaging using pulsed arterial spin labeling. J Magn Reson Imaging 2003;18:404-13.
33. Reichenbach JR, Barth M, Haacke EM, Klarhöfer M, Kaiser WA, Moser E. High-resolution MR venography at 3.0 Tesla. J Comput Assist Tomogr 2000;24:949-57.
34. Paxinos G, Watson C. The Rat Brain in Stereotaxic Coordinates. 6th ed. London, UK: Elsevier Academic Press; 2007. p. 1-463.
35. Bouma GJ, Muizelaar JP. Cerebral blood flow in severe clinical head injury. New Horizons 1995;3:384-94.
36. Schroder ML, Muizelaar JP, Kuta AJ, Choi SC. Thresholds for cerebral ischemia after severe head injury: Relationship with late CT findings and outcome. J Neurotrauma 1996;13:17-23.
37. Greve MW, Zink BJ. Pathophysiology of traumatic brain injury. Mt Sinai J Med 2009;76:97-104.
38. Engelborghs K, Verlooy J, Van Reempts J, Van Deuren B, Van de Ven M, Borgers M. Temporal changes in intracranial pressure in a modified experimental model of closed head injury. J Neurosurg 1998;89:796-806.
39. Barone FC, Ohlstein EH, Hunter AJ, Campbell CA, Hadingham SH, Parsons AA, et al. Selective antagonism of endothelin-A-receptors improves outcome in both head trauma and focal stroke in rat. J Cardiovasc Pharmacol 2000;36(Suppl 1):S357-61.
40. Yamakami I, Yamaura A. Effects of decompressive craniectomy on regional cerebral blood flow in severe head trauma patients. Neurol Med Chir (Tokyo) 1993;33:616-20.
41. Li Y, Zhang L, Kallakuri S, Zhou R, Cavanaugh JM. Quantitative relationship between axonal inury and mechanical response in a rodent head impact acceleration model. J Neurotrauma 2011;28:1767-82.
42. Tong KA, Ashwal S, Holshouser BA, Nickerson JP, Wall CJ, Shutter LA, et al. Diffuse axonal injury in children: Clinical correlation with hemorrhagic lesions. Ann Neurol 2004;56:36-50.
43. Chang EF, Claus CP, Vreman HJ, Wong RJ, Noble-Haeusslein LJ.

Heme regulation in traumatic brain injury: Relevance to the adult and developing brain. J Cereb Blood Flow Metab 2005;25:1401-17.

44. Hua Y, Nakamura T, Keep RF, Wu J, Schallert T, Hoff JT, et al. Long-term effects of experimental intracerebral hemorrhage: The role of iron. J Neurosurg 2006;104:305-12.

45. Nakamura T, Keep RF, Hua Y, Nagao S, Hoff JT, Xi G. Iron-induced oxidative brain injury after experimental intracerebral hemorrhage. Acta Neurochir Suppl 2006;96:194-8.

46. Regan RF, Panter SS. Hemoglobin potentiates excitotoxic injury in cortical cell culture. J Neurotrauma 1996;13:223-31.